



## Catalytic performance of polyvinylidene fluoride (PVDF) supported TiO<sub>2</sub> additive at microwave conditions

Huseyin Gumus<sup>1\*</sup>  

<sup>1</sup>University of Bilecik Seyh Edebali, Vocational School of Osmaneli, 11500, Osmaneli, Bilecik/Turkey

**Abstract:** TiO<sub>2</sub> is a widely used additive material to improve the properties of filtration membranes. As far as its contribution to filtration performance, TiO<sub>2</sub> acts as a catalytic agent. In this study, the catalytic activity of TiO<sub>2</sub> added PVDF flat sheets (membranes) prepared by the phase inversion method, and we tested them on the oxidation of benzyl alcohol at microwave irradiation. We investigated the structure, thermal behaviors, and morphology of samples by FTIR, TG-DTA, and SEM analysis, respectively. Contact angle measurements determined the hydrophilicity, and we observed the interaction between TiO<sub>2</sub> and PVDF chain. TiO<sub>2</sub>-added PVDF membranes had improved filtration and rejection performance. 32.4% BSA rejection was obtained with composites while it was 7.5% for the pristine membrane. We obtained 93.86% conversion and 56% selectivity with composites in a microwave-assisted batch reactor. The decomposition of the polymer increased with a 6% additive due to the catalytic effect of TiO<sub>2</sub> then, and it decreased with further loading. We obtained detailed evidence by activation energies (E<sub>a</sub>) of decomposition calculated by Kissinger's method. The microwave-assisted catalytic effect of TiO<sub>2</sub> inside the polymeric matrix promise to obtain fast, high yielded, and disposable membrane materials for catalytic reactors to in-situ production of fine chemicals.

**Keywords:** Alcohol oxidation, filtration membranes, PVDF, degradation, TiO<sub>2</sub>.

**Submitted:** August 26, 2019. **Accepted:** .March 24, 2020.

**Cite this:** Gumus H. Catalytic performance of polyvinylidene fluoride (PVDF) supported TiO<sub>2</sub> additive at microwave conditions. JOTCSA. 2020;7(2):361-74.

**DOI:** <https://doi.org/10.18596/jotcsa.610886>.

**\*Corresponding author.** E-mail: ([huseyin.gumus@bilecik.edu.tr](mailto:huseyin.gumus@bilecik.edu.tr)), Tel: (+90 228 214 1841), Fax: (+90 228 214 1342).

### INTRODUCTION

Filtration and separation membranes caused great interest in obtaining more improved performance, such as high purity, fast, and easy yields. One of the most effective routes to obtain highly efficient filtration membranes was the preparation of composites, which are a combination of two or more components. Zeolite, metal oxides, carbon-based molecular sieves, and clays were commonly used organic/inorganic filler materials into the polymer matrix (1). Researchers preferred TiO<sub>2</sub> as additive materials for filtration membranes due to their multi-functional properties such as providing thermal and physical resistance, tunable pore, and channels in addition to its photocatalytic activity (2). Degradation of organic compounds were

conducted by using TiO<sub>2</sub> at the form of suspended in solution or immobilized to support by NIPS, TIPS and spinning processes or grafting to membrane surface (3-9). Among those, suspended TiO<sub>2</sub> provided high activity, but separation from the solution and regeneration became an environmental issue, so it restricts the usage of suspension. Researchers adopted the application of the TiO<sub>2</sub>-immobilized polymer matrix, and they used composite membranes, mainly separation of particles, degradation of organic contaminants, production of fine chemicals, and bacterial removal. Researchers used Ag particles combined with TiO<sub>2</sub>-Perlite for the degradation of methylene blue removal under UV light radiation (10). Hydroxyl groups that emerged on the surface of composites turned to hydroxyl radicals when UV

radiation exposed to them, and these induced to the decomposition of organic dye, waste, and bacteria.

Some authors also prepared TiO<sub>2</sub> dispersed filtration membranes and investigated in terms of additive size, additive ratio, as far as they met the composition, and coagulation conditions (11,12). An extended summary was reported by Mendret et al. about TiO<sub>2</sub>-deposited polymers, particularly for the combination of TiO<sub>2</sub> and PVDF (13). TiO<sub>2</sub> provided excellent hydrophilicity and permeation to filtration membranes. Mainly, embedded membranes having nanosized particles performed better antifouling properties compared with their pristine forms (14,15). Self-cleaning ability is related to the photocatalytic activity of TiO<sub>2</sub> immobilized on the membranes.

Some authors prepared additive contained polymeric or ceramic matrixes to achieve instant reaction of substrates during filtration as catalytic membrane reactors. The common advantages of these systems are easy reaction and separation with low cost and reusability. Some researchers conducted phenol hydroxylation and p-aminophenol production by hydrogenation of p-nitrophenol on ceramic membrane reactors with high yield (16,17). For the oxidation of phenol with peroxide, the authors used a packed bed reactor consisting of FeZSM-5 zeolite immobilized on silicon carbide (SiC) foam catalyst. At 60 °C and 1 mL min<sup>-1</sup> flow, the researchers obtained 3.4 kJ mol<sup>-1</sup> activation energy of phenol degradation with 95 h<sup>-1</sup> turnover frequency. These kinds of systems require polymeric materials that have high physical and chemical resistance. PVDF is known for its high chemical, physical, and thermal resistance, and we see its use for chemical reactors and applications using UV light irradiation (18).

On the other hand, TiO<sub>2</sub> can be used to dispose of polluting polymers, organics, and polymeric materials economically, for instance, the application of polyethylene degradation by PAM grafted TiO<sub>2</sub> (19). A group of researchers investigated the photocatalytic degradation of the polystyrene matrix by the immobilized TiO<sub>2</sub>, and they recorded a decrease at the molecular weight of the polymer (20). Thermal behaviors are also essential indicators about the resistance capacity of polymer, and those provide information about the interaction of additive with a polymer matrix (21).

In general, under appropriate rates, TiO<sub>2</sub> contributed better thermal stability to the polymer matrix. Polymer coated by nucleated additives induces crystalline formation on polymer during the phase separation (22–24). According to literature overviewed, TiO<sub>2</sub> immobilized/embedded/

coated polymeric composite membranes have better thermal resistance in addition to improved flux, rejection, and other filtration properties compared with pristine forms.

In this study, we aimed to determine the catalytic and thermal oxidative degradation properties and their filtration performance of TiO<sub>2</sub>-blended PVDF membranes prepared at different mass ratios. In distinct energy supply, we conducted the oxidation experiments of benzyl alcohol in a microwave radiated batch reactor cooled with a condenser. We also investigated the polymer decomposition behaviors of TiO<sub>2</sub> (inside the structure) by detailed thermal analysis and decomposition enthalpies calculated by the Kissinger's method. We evaluated whether these are usable or not as a catalytic membrane at microwave conditions to get a fast and environmentally friendly design.

We tested only 0.5-4% TiO<sub>2</sub> contained filtration membranes in terms of filtration performances due to the inconvenience of the filtration ability of high loading composites. We also investigated the effect of additive ratio and dispersion of particles on the membrane properties on the heat resistance of composite membrane and disposal method for polymeric waste by the obscured thermal-oxidative activity of TiO<sub>2</sub> in addition to its well-known photocatalytic activity.

## EXPERIMENTAL SECTION

### Materials

Polyvinylidene fluoride, PVDF (Solef 6010), was used as the polymer material without any purification with N, N-dimethylformamide (DMF; Sigma Aldrich) as a solvent and distilled water. For the synthesis of TiO<sub>2</sub>, titanium(IV) isopropoxide, Ti[OCH(CH<sub>3</sub>)<sub>2</sub>]<sub>4</sub> (284.22 g/mol, 97% w/w, 0.960 g/mL), sodium chloride, NaCl (58.44 g/mol), ethanol, C<sub>2</sub>H<sub>5</sub>OH (46.06 g/mol, 0.789 g/mL) were purchased from Sigma-Aldrich. We used a model protein-solution with bovine serum albumin, BSA (MW: 66000 Da, ≥98% purity, Sigma Aldrich) with boric acid, H<sub>3</sub>BO<sub>3</sub> (MW: 61.83 g/mol, Sigma-Aldrich), ortho-phosphoric acid, H<sub>3</sub>PO<sub>4</sub> (MW: 98 g/mol, Sigma-Aldrich) and acetic acid, CH<sub>3</sub>COOH (MW:60.05 g/mol, 99.7%, Sigma-Aldrich) as acidity adjustment. We procured benzyl alcohol and hydrogen peroxide (30% w/v) from Panreac.

### Preparation of TiO<sub>2</sub> and TiO<sub>2</sub>-PVDF composite membranes

We prepared the TiO<sub>2</sub>-blended PVDF membranes by wet-phase inversion technique determined in a report (25). To synthesize TiO<sub>2</sub> particles, titanium(IV) isopropoxide (0.11 mol/L) and NaCl solution (%1 w/w) were mixed in a round-bottomed flask and stirred with a magnetic stirrer for ten minutes. We then left the obtained slurry to

rest for approximately 12 hours. It was then filtered and washed with hot ethanol and water. The precipitate was dried at 60 °C and ground to powder at the size of 5-100 µm. An appropriate amount of dry solid was weighed and dissolved in DMF by ultrasonication. We added it to the polymer solution obtained by dissolving PVDF (1.6 g) in DMF (10 mL) as a 14% mass ratio in terms of polymer to solvent. The mixture of PVDF/DMF/TiO<sub>2</sub> was stirred at 250 rpm at 65 °C for 12 hours, and we kept it in the ultrasonication bath for 10 minutes to obtain a homogeneous dispersion. The mixture was waited for a time to prevent air

bubbles and cast on to a flat surface (15 cm x 15 cm) uniformly by a 300 µm casting knife at 25 °C. After exposure to air for 10 seconds, we quickly immersed the glass plate into the coagulation bath. Figure 1 represents the steps of preparation. Membranes were dried and used for characterization and alcohol oxidation. We stored the filtration membranes in distilled water for filtration experiments. Membranes contain TiO<sub>2</sub> at the rate of 0, 0.5, 1, 2, 4, 6, and 8% according to the total mass of combination were determined as PVDF, T05-P, T1-P, T2-P, T4-P, T6-P, and T8-P respectively.

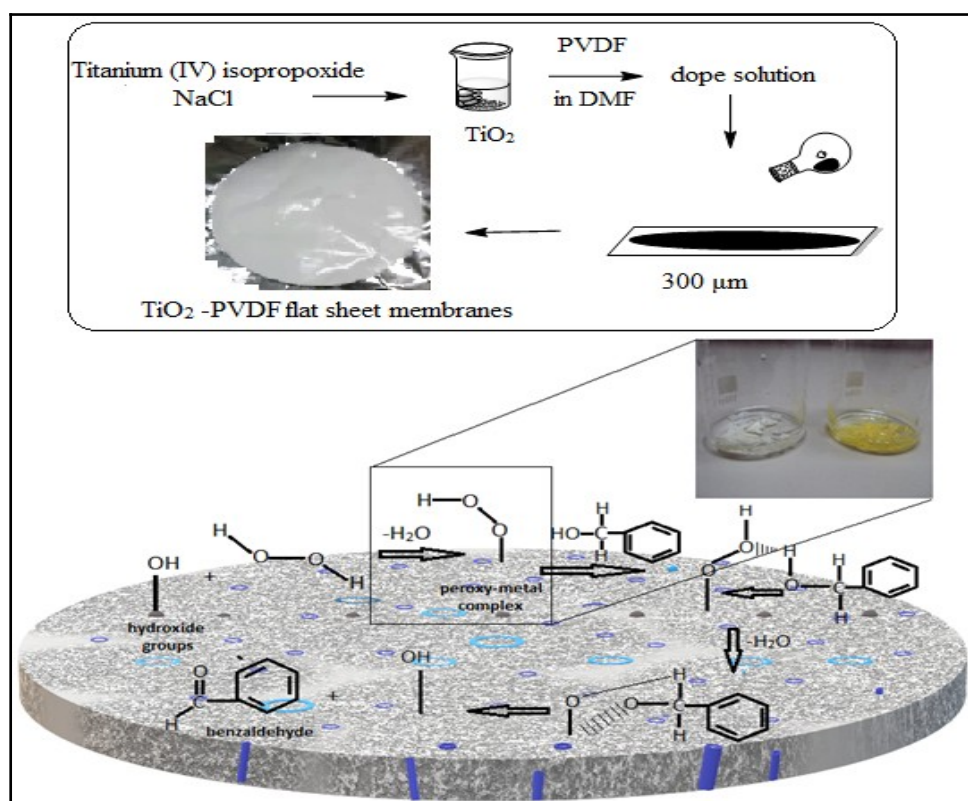


**Figure 1:** Illustration for the preparation of TiO<sub>2</sub>-PVDF and peroxy metal complex.

### Characterization of TiO<sub>2</sub> and TiO<sub>2</sub>-PVDF composite membranes

We recorded the FTIR spectra of TiO<sub>2</sub> and membranes in the region between 4000 and 650 cm<sup>-1</sup> by a Perkin-Elmer FTIR spectrometer. Thermal stability and content of inorganic matter of samples were investigated by the thermogravimetric analyzer (TG-DTA, Exstar 7020) under the aerial atmosphere. We have adjusted typical conditions as about 5-7 mg of sample weight and 20 °C/min heating rate. We evaluated the thermal decomposition effect of TiO<sub>2</sub> to polymer, and we heated the samples in 50-1000 °C temperature range by 5, 10, 15, 20 and 30 °C/minute heating rates. The hydrophilicity of membranes was analyzed by a KSV Attention contact angle analyzer (Finland) at 25 °C temperature. The morphology of membranes was

examined by Carl Zeiss ULTRA Plus SEM device (Germany) at 10 kV. We photographed the cross-section images of samples broken in liquid nitrogen. As a model contaminant, we used BSA to determine membrane performance. We have analyzed the absorbance of the contaminant with a UV-visible spectrophotometer (PG Instruments, T80) at 280 nm wavelength (24).

We determined the water uptake capacity (WU) of membranes stored in water by measuring the weight of wet ( $W_w$ ) and dried ( $W_d$ ) membranes dried at 40 °C in a vacuum oven for 2 hours. We used Equation 1 to calculate.

$$WU(\%) = \frac{W_w - W_d}{W_w} \times 100$$

(1)

Pore percentage called as membrane porosity (PO) was calculated by following eq. (2):

$$PO(\%) = \frac{W_w - W_d}{dA\delta} \times 100 \quad (2)$$

Where d is the density of deionized water at 25 °C (the temperature of studies conducted), A is the area of the membrane (cm<sup>2</sup>) and  $\delta$  is the thickness of wet membrane (cm).

### Water flux, rejection and antifouling performances of composite membranes

We measured the pure water flux (PWF) performances of membranes by collecting the permeated water (L/m<sup>2</sup>h) at ultrafiltration cross-flow membrane cell. We adjusted the transmembrane pressures (TMP) as 100, 200, and 300 kPa after pre-conditioning of membranes for 1-3 h (26-27). We calculated WF by Equation (3) (28).

$$WF = \frac{V}{At} \quad (3)$$

where V is the volume of water-permeated (L), A is the surface of the membrane (1.7x10<sup>-3</sup> m<sup>2</sup>), and t represents the sampling time (h). Compaction factor (CF) means the physical resistance of membranes, and we calculated that by dividing the initial WF<sub>i</sub> value by constant WF<sub>c</sub> value. We prepared the 0.5 g/L BSA solution with phosphate buffer (0.01 mol/L, pH:7.4) and filtered it at 200 kPa. We determined the concentration of BSA in collected permeate with a UV-Vis spectrophotometer and calculated the rejection performance with Equation (4).

$$R(\%) = \left( 1 - \frac{C_p}{C_f} \right) \times 100 \quad (4)$$

Where C<sub>p</sub> and C<sub>f</sub> stand for the concentration of initial and final solutions of BSA, respectively.

### Catalytic activity experiments

A previous study investigated the catalytic activities on benzyl alcohol conversion of TiO<sub>2</sub>-PVDF samples in a batch reactor (29) We put 0.02 g of TiO<sub>2</sub>-PVDF membrane pieces (1.5x1.5 cm) kept in benzyl alcohol for the diffusion of the substrate into a 50 mL reaction cup along with 1 mmol benzyl alcohol and 1 mmol H<sub>2</sub>O<sub>2</sub>. We then applied 500 W microwave radiation in a cooled microwave oven for 8 minutes. We analyzed a sample with GC, taken from the reaction mixture with a syringe (without any filtration). We washed the pieces of the membrane with acetone and used these samples three times. We performed the calculation of conversion and benzaldehyde selectivity of samples according to Equations 6 and 7. We used powder TiO<sub>2</sub> as a catalyst with the same reaction conditions. We filtered the sample taken from the powder catalyst with a syringe filter before injection to the column.

$$Conversion\% (C\%) = \frac{C_{alcohol(initial)} - C_{alcohol(final)}}{C_{alcohol(initial)}} \times 100 \quad (6)$$

$$Selectivity\% (S\%) = \frac{\text{Amount of benzaldehyde}}{\text{Amount of all products}} \times 100 \quad (7)$$

## RESULTS AND DISCUSSION

### FTIR analysis of TiO<sub>2</sub> and TiO<sub>2</sub>-PVDF membranes

We carried out FTIR analyses to understand the interaction of TiO<sub>2</sub> and the polymer chain. We have observed satisfactory evidence proving the blend of TiO<sub>2</sub> with a chain structure of PVDF in Figure 2.

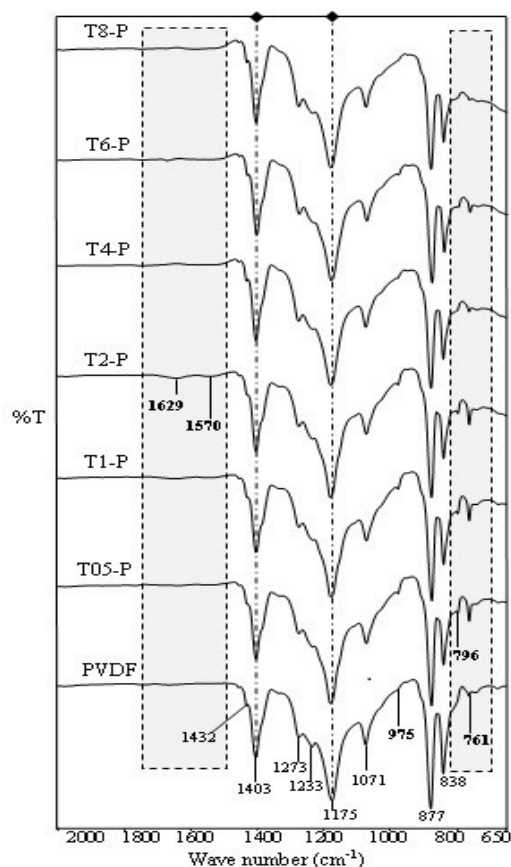


**Figure 2:** FT-IR spectra of TiO<sub>2</sub>-PVDF samples.

$\alpha$ -phases of PVDF ascribed with 761, 796, and 975 cm<sup>-1</sup> bands disappeared with increasing TiO<sub>2</sub> amount. This outcome indicated the formation of an amorphous structure with increased TiO<sub>2</sub> loading. We could see the superimposed FTIR bands of pristine and composites at the high wavenumber, but deviations emerged at the bands of 761, 976, and 1233 cm<sup>-1</sup> due to increasing TiO<sub>2</sub>. We observed characteristic CH<sub>2</sub> and CF<sub>2</sub> stretching vibrations at 1403, and 877-1175 cm<sup>-1</sup>,

respectively, and CF stretching bands of the PVDF chain at 1071 cm<sup>-1</sup>. We obtained an essential indication for TiO<sub>2</sub> and PVDF interaction with the band at ca. 1570 cm<sup>-1</sup> indicating the presence of OH groups on TiO<sub>2</sub> bonding with the PVDF chain (30-32). The band at 1629 cm<sup>-1</sup> emerged due to the presence of the Ti-O-Ti structure and indicated possible hydrogen bonding between the oxygen of TiO<sub>2</sub> and fluorides of PVDF (23-25, 33). Figure 3 represents the possible bonding.

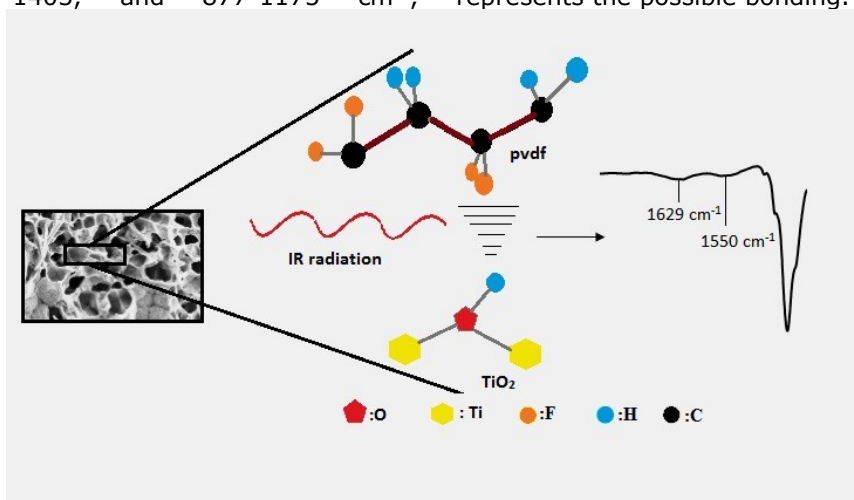


**Figure 3:** Estimated bonding of Ti-O-Ti with PVDF chain.

### Morphology of composites

Figure 4 presents the cross-section SEM images of the composites to understand better the effect of  $\text{TiO}_2$  addition on the structure of the membrane.

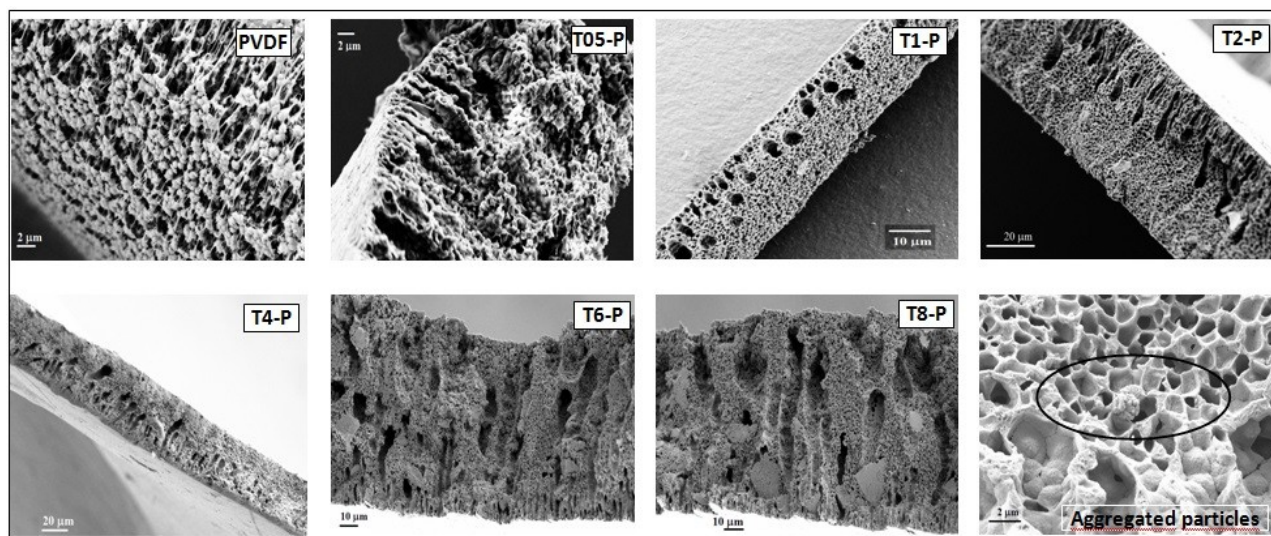


**Figure 4:** SEM images of  $\text{TiO}_2$ -PVDF samples.

Bare PVDF and additive contained samples showed different morphology as mainly symmetric and asymmetric forms. PVDF membrane structure, having large holes among the polymer clusters, became sponge-like as could be seen at the image of T1-P with macroscopic voids. We observed that, for T2-P and T4-P, the uniform membrane structure consisting of finger-like pores connected to the sponge side. In general, we obtained appropriately dispersed particles for the samples which have finger-like pores, despite the aggregated  $\text{TiO}_2$  remnants available among the pores. We also observed a severe deviation from uniformity for samples containing additive amounts at 6% and further.

Furthermore, a high amount of additive pressed the micro-pores and channels, which determine the permeation and rejection performances of membranes. Additive, along with the solvent type, has a prominent effect on the formation of membrane structure such as a sponge, macro, and finger-like properties according to the affinity of water (11). Researchers reported the crystalline form of  $\text{TiO}_2$  and DMF as a solvent to result in a

thicker structure of hollow fiber membranes (34-35).

High water affinity of  $\text{TiO}_2$  accelerated to mixing of coagulation water with polymer solvent (DMF) during phase inversion. Thus, the solvent separation occurred faster than additive-free samples. Due to the hydrophobic nature of PVDF, polymeric lumps formed containing large holes at the bare PVDF membrane. Structural changes observed by SEM images were compatible with the permeation results presented in Figure 6. With the further amount of  $\text{TiO}_2$  deposition, convenient finger-like structures of membrane began to turn on dense sponge-like with large agglomeration. 4%  $\text{TiO}_2$  amount was concluded as a maximum ratio to obtain sufficient filtration behavior.

### Thermal analysis and thermal catalytic activity of composites

The thermal stability of samples was analyzed by TG and DTA to understand the effect of additive on to polymeric structure at the temperature ranges of 30-1000 °C (Figure 5). Ash contents obtained for the PVDF and  $\text{TiO}_2$  contained PVDF samples were different from the additive ratios.

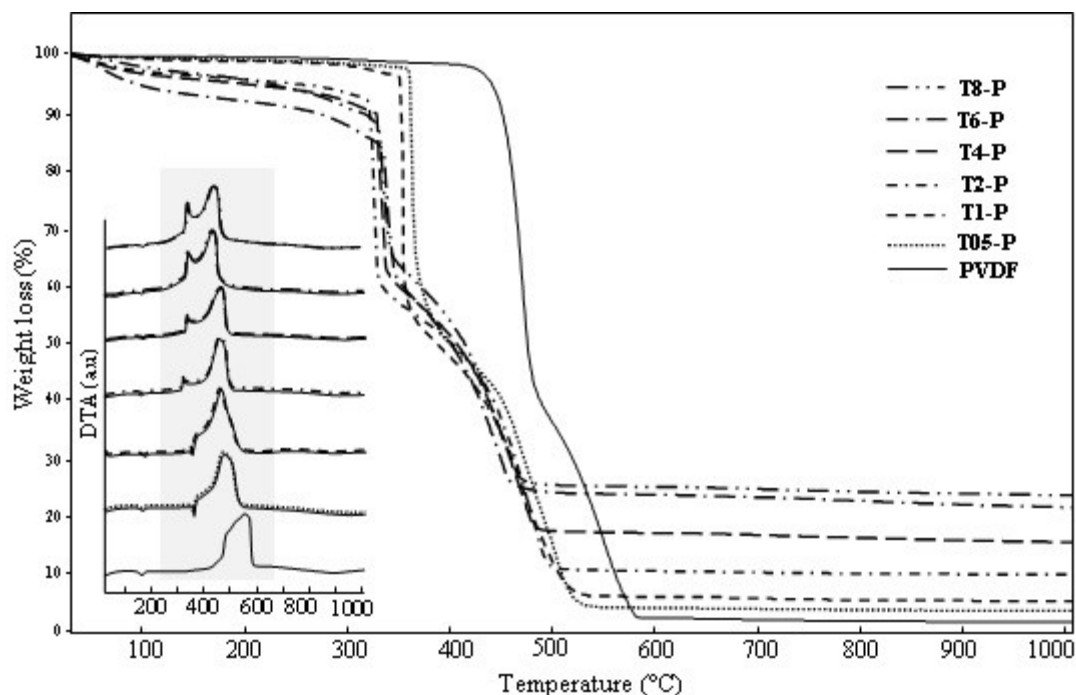


**Figure 5:** TG and DTA curves of TiO<sub>2</sub>-PVDF samples.

During the calculation of the dope solution, only polymer and additives burned along with a small amount of solvent in the thermal analyzer. After the exposure of samples to heat, the remaining weight indicated to TiO<sub>2</sub> inside the membranes. The process burned all of the organic contents of the polymer. In Figure 5, we recorded that the degradation of neat PVDF started at 470 °C, whereas the degradation temperatures of composites were between 348-339 °C, which was a lower temperature than neat PVDF. We know that TiO<sub>2</sub> deposition onto polymeric support has

two opposite effects for the thermal behaviors of the samples. (1) TiO<sub>2</sub> may cover the surface of the polymer and improve the thermal resistance of the composite by protecting the polymer from direct exposing of oxygen or (2) thermal catalytic oxidation of TiO<sub>2</sub> may be dominant, and it may increase the thermal degradation of the organic structure due to thermal catalytic effect of TiO<sub>2</sub> at high temperatures (36). Patra and coworkers explained the increasing thermal resistance for the additive containing samples due to the escape of the radicals (20).

**Table 1:** Thermal behaviors of TiO<sub>2</sub>-PVDF samples.

| Sample | t <sub>onset</sub> (°C) | t <sub>max</sub> (°C) | t <sub>endset</sub> (°C) | t%10 (°C) |
|--------|-------------------------|-----------------------|--------------------------|-----------|
| PVDF   | 374                     | 470                   | 593                      | 450       |
| T05-P  | 351                     | 362                   | 546                      | 361       |
| T1-P   | 328                     | 348                   | 565                      | 347       |
| T2-P   | 328                     | 348                   | 541                      | 347       |
| T4-P   | 300                     | 326                   | 523                      | 321       |
| T6-P   | 312                     | 332                   | 503                      | 320       |
| T8-P   | 305                     | 339                   | 494                      | 288       |

Rather than shielding, the catalytic thermal decomposition effect of additives dominated, and it decreased the on-set and max temperatures of TiO<sub>2</sub> contained samples (Table 1). Thermal degradation of samples accelerated, and end-set temperatures were recorded between 494-565 °C, whereas it was 593 °C for neat PVDF. Reduced degradation temperature values of additive containing samples are clear indicators for the thermal decomposition effect of TiO<sub>2</sub>. Differential

thermal analysis (DTA) curves confirmed the results of the thermal degradation of the polymeric structure (Figure 5). Exothermic peaks of PVDF at 440-560 °C emerged after the burning of organic components was observed at lower temperatures with increasing TiO<sub>2</sub> amounts. Besides, we observed for T4-P, T6-P, and T8-P one more exothermic peak, which represents degradation, and these were different from PVDF. An endothermic peak at around 170 °C may

correspond to the melting point of polymer (37). Increasing of additive resulted in a decrease at the crystallinity of polymer, and TiO<sub>2</sub> clusters started to agglomerate differently. A disordered structure meant weakened binding of OH groups on TiO<sub>2</sub> with a PVDF chain pointed by FTIR results (see the section about FTIR). That induced the degradation effect of TiO<sub>2</sub> at high temperatures. We conducted the thermal analysis of samples to demonstrate the degradation effect of the additive at high heating rates: 5, 10, 15, 20, 30 °C/minute, and activation energy of samples were calculated by Kissinger’s method (38) according to TG results obtained under air. We calculated the activation

energies of degradation by linearization of  $\beta/T_{max}^2$  versus  $1/T_{max}$  according to Equation 1.

$$\left(\frac{\beta}{T_{max}^2}\right) = \left(\frac{AR}{E_a}\right) - \frac{E_a}{RT_{max}} \tag{1}$$

Where  $\beta$  is the heating rate, A is a pre-exponential factor, E<sub>a</sub> is the calculated activation energy for degradation of samples, and R is the universal gas constant. By using the maximum degradation occurred, we calculated the activation energy values. We presented T<sub>max</sub> and E<sub>a</sub> values calculated by the mentioned method in Table 2.

**Table 2:** T<sub>max</sub> and degradation energy values of TiO<sub>2</sub>-PVDF samples.

| TiO <sub>2</sub> content (Wt. %) | $\beta$ (°C/min) |     |     |     |     | E <sub>a</sub> (kJ/mol) |
|----------------------------------|------------------|-----|-----|-----|-----|-------------------------|
|                                  | 5                | 10  | 15  | 20  | 30  |                         |
| -                                | 447              | 470 | 444 | 460 | 482 | 193.5                   |
| 0.5                              | 342              | 362 | 334 | 345 | 353 | 135.8                   |
| 1                                | 340              | 348 | 355 | 365 | 378 | 138.5                   |
| 2                                | 335              | 347 | 348 | 355 | 374 | 136.9                   |
| 4                                | 314              | 326 | 337 | 347 | 366 | 95.1                    |
| 6                                | 329              | 332 | 336 | 343 | 351 | 217.4                   |
| 8                                | 334              | 339 | 339 | 344 | 351 | 305.5                   |

The E<sub>a</sub> of PVDF was 193.5 kJ/mol, and it was observed as 136.9 and 95.1 kJ/mol for T2-P and T4-P respectively under the air atmosphere. Thermal properties of composites given in Table 1 and Figure 5 are compatible with the activation energy values. In general, activation energy decreased with an increased amount of additive, relatively with changes of T<sub>onset</sub> and T<sub>max</sub> values. E<sub>a</sub> values provided clear information about how the additive rate affected the degradation process. To bare TG results, very little increase was observed for max decomposition as can be assumed negligible. But 217.4 and 305.5 kJ/mol E<sub>a</sub> values recorded for T6-P and T8-P respectively indicated that further loading of additive prevented the

degradation of the polymer due to the shielding effect of agglomerated spherical TiO<sub>2</sub> clusters. The thermal stability of PVDF decreased because of the thermal oxidative effect of TiO<sub>2</sub> until the 4% TiO<sub>2</sub>, which is the final sufficient composition as a filtration membrane. After that activation energy increased, the shielding effect became dominant when the 6% and further additive loadings. We have observed competition between shielding and thermal decomposition effects until the 6% additive.

**Filtration Performances of composites**

We tested the water flux (WF) of membranes cross-flow filtration system (see Figure 6).

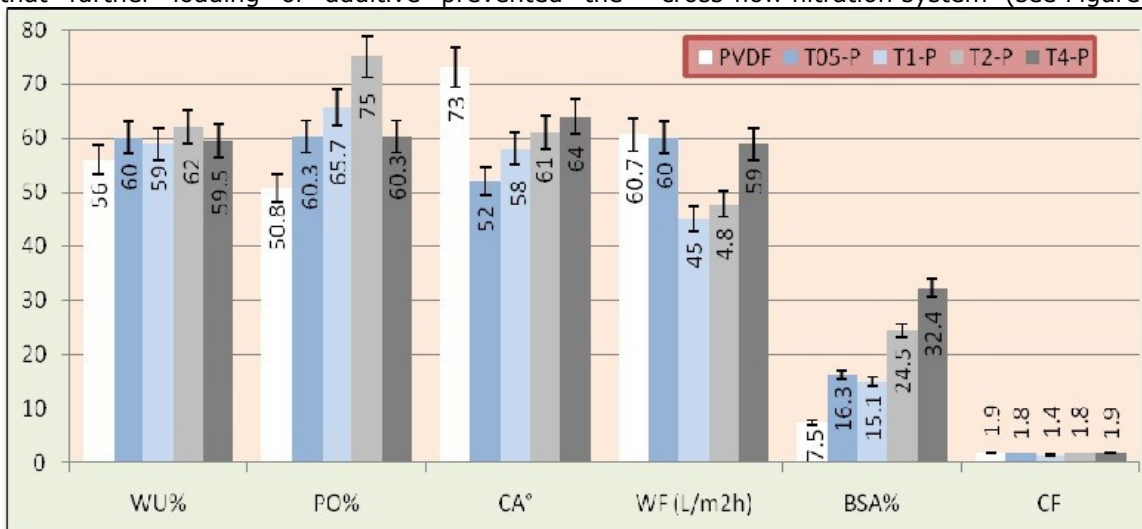


**Figure 6:** Filtration performances of PVDF and TiO<sub>2</sub>-PVDF samples.

WF values decreased with increasing hydrophilic TiO<sub>2</sub> additive, which is controversial with the phenomena of the more hydrophilic, the more improved in water flux (39). Water permeation is commonly not only depending on hydrophilicity but also porosity, thickness, and water uptake (11). T2-P showed the highest porosity and water uptake for T2-P, which were 75% and 62%, respectively. Porosity and water uptake values of composite membranes were higher than that of the pristine PVDF membrane. As a controversy, water permeation of composites was lower than the PVDF membrane. In that case, we understood that the thickness and pore size determined the permeation performances of membranes. We saw the formation of a large number of small pores during phase separation. That was result of accelerated process induced by hydrophilic additives with increasing porosity. A relative change was observed among the porosity and water uptake values. Porosity and water uptake of PVDF were 50.8% and 56% respectively. High porosity with low water uptake of composites was also another proof for the existence of small pores. Effect of hydrophilic additive was confirmed by contact angle measurements. It is known that the smaller contact angle means the better hydrophilicity (40). Lower contact angle values were obtained for all samples compared with contact angles of PVDF (73°). Roughness of membrane surface suppressed the hydrophilic character of additive with further TiO<sub>2</sub> loading ratios. Due to agglomerated particles contact angles values were began to rise. Thick skin layer had a respectable effect on filtration performance and physical properties of membranes. Formation

of a thicker and stuck layer was induced by increasing viscosity of dope solution. That was confirmed by lower compaction values of membranes. Denser composition of composite membranes performed lower compaction values. We have concluded that the type and amount of additive have a considerable effect on the pores, voids, and channels of all structures with physical effects. BSA rejection performances were investigated to interpret structural characteristics of membranes. Dense structure of membrane provided an advantage as high rejection performance. 32.4% BSA rejection values was obtained for T4-P sample while it was only 7.5% for PVDF. Permeable polymeric lumps determined in SEM images of PVDF (Figure 4), provided low rejection although moderate flux. New structures formed by TiO<sub>2</sub> addition presented tightened skin which was beneficial for filtration and higher rejection. Generally it was known that particle accumulation on the surface occurs by electrostatic interaction between surface and particles (38). Flux recovery values a little reduced due to the interaction of BSA and surface groups. The roughness of the membrane promoted to an accumulation of rejected particles on the surface of the membrane.

#### The catalytic activity of composites

We have used a round-bottomed flask to test the catalytic activity of TiO<sub>2</sub>-PVDF flat sheets on benzyl alcohol oxidation. We adjusted the alcohol and peroxide ratio to 1:1 with 0.06 g catalyst without solvent. We put the reaction flask cooled with a condenser into the microwave furnace. Table 3 shows the results of optimization experiments.

**Table 3:** Conversion and benzaldehyde selectivity of TiO<sub>2</sub>-PVDF composite samples.

| Entry   | Catalyst (amount, g)    | Temperature (°C) | Reaction Time (min.) | Conversion-selectivity (%) |
|---------|-------------------------|------------------|----------------------|----------------------------|
| 1       | -                       | R.T.             | 240                  | -                          |
| 2       | -                       | 80               | 240                  | -                          |
| 3       | -                       | 80*              | 8                    | -                          |
| 4       | TiO <sub>2</sub> (0.06) | R.T.             | 240                  | -                          |
| 5       | TiO <sub>2</sub> (0.06) | 80               | 240                  | 26.2-33.5                  |
| 6       | TiO <sub>2</sub> (0.06) | 80*              | 8                    | 86.0-4.4                   |
| 7       | T2-P (0.06)             | R.T.             | 240                  | -                          |
| 8       | T2-P (0.06)             | 80               | 240                  | 25.5 - 45                  |
| 9       | T05-P (0.06)            | 80*              | 8                    | -                          |
| 10      | T1-P (0.06)             | 80*              | 8                    | 53.15 -21.4                |
| 11      | T2-P (0.06)             | 80*              | 8                    | 67 - 29                    |
| 12      | T4-P (0.06)             | 80*              | 8                    | 62.9-45.4                  |
| 13      | T6-P (0.06)             | 80*              | 8                    | 66.6-16.2                  |
| 14      | T8-P (0.06)             | 80*              | 8                    | 27-26                      |
| 15      | T4-P (0.02)             | 80*              | 8                    | 70.7 - 36                  |
| 16      | T4-P (0.04)             | 80*              | 8                    | 76.9 - 5.9                 |
| 17      | T4-P (0.08)             | 80*              | 8                    | 54 - 20                    |
| 18**0   | T4-P (0.06)             | 80*              | 8                    | 48.46 - 4.35               |
| 19**0.2 | T4-P (0.06)             | 80*              | 8                    | 59.4 - 34.3                |
| 20**0.4 | T4-P (0.06)             | 80*              | 8                    | 62.5 - 48                  |

|          |             |     |   |              |
|----------|-------------|-----|---|--------------|
| 21**0.6  | T4-P (0.06) | 80* | 8 | 56.37- 56    |
| 22**0.8  | T4-P (0.06) | 80* | 8 | 56.5 - 56    |
| 23**1    | T4-P (0.06) | 80* | 8 | 73 - 38.7    |
| 24**1.5  | T4-P (0.06) | 80* | 8 | 93.86 - 5.84 |
| 25-300W  | T4-P (0.06) | 80* | 8 | 76 - 17      |
| 26-700W  | T4-P (0.06) | 80* | 8 | 70 - 36      |
| 2. reuse | T4-P (0.06) | 80* | 8 | 63.4 - 74    |
| 3. reuse | T4-P (0.06) | 80* | 8 | 80 - 37      |
| 4. reuse | T4-P (0.06) | 80* | 8 | 59 - 35      |

We carried out the reaction in a 50 mL flask with a condenser in a 500 W microwave, with 1 mmol H<sub>2</sub>O<sub>2</sub> and 1 mmol benzyl alcohol ratio unless otherwise stated. We introduced the mixture to an HP-5 column for GC analysis.

\*: in microwave radiation.

\*\* :H<sub>2</sub>O<sub>2</sub>: Benzyl alcohol ratio (mol)

We investigated the effects of various parameters on the reaction yield. A high conversion with high selectivity was a considerable result. A satisfactory result was obtained with 0.06 g T4-P sample. That was directly related to easy transferring of substrate to active sites of catalyst. Structural properties such as pore distribution, pore radius, cross-section thickness, and the additive were essential determiners of substrate flow and, consequently, the reaction yield. Moderate pores provided easy transferring of substrate conversely, pressed structure complicated transportation. As could be seen, T4-P has a more hydrophobic character inferred from its high contact angle and low water uptake capacities. That makes it more attractive to organic substrate. The more organic substrate diffused inside the active sites give the more selectivity. On the other hand, selectivity performance of T4-P may due to its prevention effect of over peroxide transferring due to its hydrophobicity. Experiments conducted to

understand peroxide ratio at the reaction yield supported this estimation. High conversion but low selectivity was obtained with increased peroxide ratio. That meant that benzyl alcohol was converted into other oxidation products. Changes of peroxide alcohol ratio may resulted in different products (39). 0.4 (H<sub>2</sub>O<sub>2</sub>: benzyl alcohol molar ratio) was considered as optimum peroxide amount. The results of 0 and 0.2 ratios specified stoichiometric peroxide shortage. Reason for low selectivity, although increased peroxide ratio may be decomposition or transferring problem of peroxide (29). The catalyst amount had a direct effect on the product type. Highest conversion was obtained when the TiO<sub>2</sub>-PVDF was 0.04 g but low selectivity. It decreased when it was further than 0.06 g. Increase at the conversion was related with high amount of catalysis. However, the exact reason may be over-oxidation of benzaldehyde or direct conversion of benzoic acid to its by-products (see Figure 7) (41).

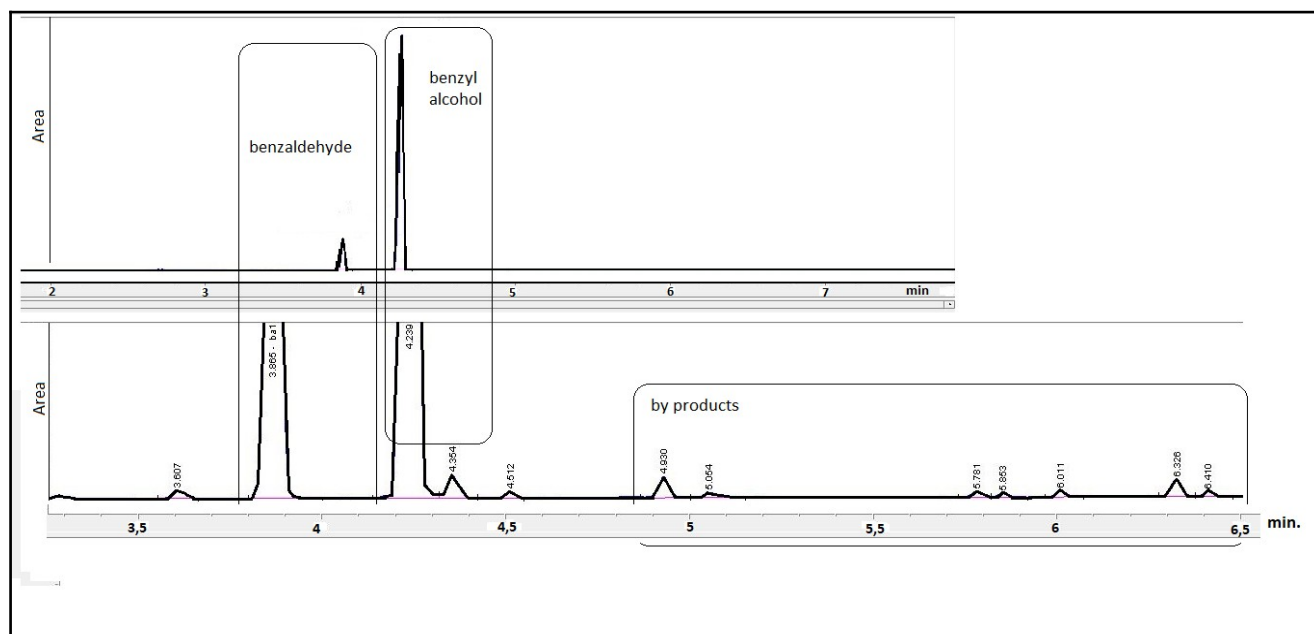


**Figure 7:** GC peaks of benzaldehyde and other products.

In this study, we saw that complex peroxy-metal structures formed as a result of the interaction of hydrogen peroxide and metals on the catalyst (Figure 1). During the oxidation, peroxide decomposed quickly in the presence of a high amount of catalyst to give active hydroxyl radicals. Even though a high number of hydroxyl radicals desired to the conversion of a substrate, the formation of active reactants quickly may cause over oxidation of reactant, consequently low selectivity. We did not observe notable results with different microwave radiation. (see Table 3). We separated TiO<sub>2</sub>-PVDF pieces from the mixture and washed with acetone, then reused three times. Washing with organic solvent wiped off all organic residues and opened the channels. However, the structure gets shrunk with further reuse due to microwave radiation. Benzyl alcohol conversion and benzaldehyde selectivity decreased gradually, with ongoing usage. TiO<sub>2</sub> embedded PVDF flat sheets performed moderate yield in addition to easy usage, low cost, and fast results at solvent-free area. The advantages of easy separation from the reaction mixture without solvent and reusability were considered remarkable output for oxidation reactions.

## CONCLUSION

We combined the well-known advantages of TiO<sub>2</sub> additive on PVDF membranes to obtain sufficient, fast, and environmentally friendly chemical production systems with microwave radiation. TiO<sub>2</sub> provided improvement filtration and better BSA rejection by increasing hydrophilicity of the polymeric matrix for almost all membranes. 4% TiO<sub>2</sub> contained samples presented 32.4% BSA rejection while it was only 7.5% for PVDF. TiO<sub>2</sub> interaction with PVDF ascribed by the FTIR bands of Ti-OH and Ti-O-Ti vibrations.

We found a clear insight by the thermal behaviors of TiO<sub>2</sub> on the membrane structure, which are not available in the primary thermal analysis results. Activation energies belong to polymeric decomposition were recorded at different heating rates. Unlike preventing effect, TiO<sub>2</sub> induced thermal decomposition of the polymer due to its catalytic activity, especially at high temperatures.

TiO<sub>2</sub>-PVDF membrane pieces were used as a microwave-induced catalyst to obtain benzaldehyde from benzyl alcohol in a batch reactor. 62.9% conversion and 45.4% selectivity with the T4-P sample. We investigated the possibility of faster and cleaner in-situ production of fine chemicals on the TiO<sub>2</sub>-catalyzed filtration system combined with microwave radiation. TiO<sub>2</sub>-added PVDF self-recyclable membranes have a high potential to the production of chemicals on

filtration systems with microwave energy, besides their well known hydrophilic, antifouling, and high rejection properties.

## ACKNOWLEDGEMENTS

This research did not receive any specific grant from funding agencies in the public, commercial, or not for profit sectors.

## Availability of the data

The processed data required to reproduce these findings are available to download from [<https://data.mendeley.com/datasets/w2678cnzsg/1>].

## REFERENCES

1. Xu Z, Wu T, Shi J, Teng K, Wang W, Ma M, et al. Photo catalytic antifouling PVDF ultra filtration membranes based on synergy of graphene oxide and TiO<sub>2</sub> for water treatment. *Journal of Membrane Science*. 2016;520:281–93.
2. Nor NAM, Jaafar J, Ismail AF, Mohamed MA, Rahman MA, Othman MHD, et al. Preparation and performance of PVDF-based nanocomposite membrane consisting of TiO<sub>2</sub> nanofibers for organic pollutant decomposition in wastewater under UV irradiation. *Desalination*. 2016;391:89–97.
3. Laohaprapanon S, Vanderlipe AD, Doma BT, You SJ. Self-cleaning and antifouling properties of plasma-grafted poly(vinylidene fluoride) membrane coated with ZnO for water treatment. *Journal of the Taiwan Institute of Chemical Engineers*. 2017;70:15–22.
4. Munoz-Bonilla A, Kubacka A, Fernandez-Garcia M, Ferrer M, Fernandez-Garcia M, Cerrada ML. Visible and ultraviolet antibacterial behavior in PVDF-TiO<sub>2</sub> nanocomposite films. *European Polymer Journal*. 2015;71:412–22.
5. You SJ, Semblante GU, Lu SC, Damodar RA, Wei TC. Evaluation of the antifouling and photo catalytic properties of poly(vinylidene fluoride) plasma-grafted poly(acrylic acid) membrane with self-assembled TiO<sub>2</sub>. *Journal of Hazardous Materials*. 2012;237–238:10–9.
6. Kim BS, Lee J. Macroporous PVDF/TiO<sub>2</sub> membranes with three-dimensionally interconnected pore structures produced by directional melt crystallization. *Chemical Engineering Journal*. 2016;301:158–65.
7. Wang Q, Wang X, Wang Z, Huang J, Wang

- Y. PVDF membranes with simultaneously enhanced permeability and selectivity by breaking the tradeoff effect via atomic layer deposition of TiO<sub>2</sub>. *Journal of Membrane Science*. 2013;442:57–64.
8. Zhang X, Wang Y, You Y, Meng H, Zhang J, Xu X. Preparation, performance and adsorption activity of TiO<sub>2</sub> nanoparticles entrapped PVDF hybrid membranes. *Applied Surface Science*. 2012;263:660–5.
9. Shi F, Ma Y, Ma J, Wang P, Sun W. Preparation and characterization of PVDF / TiO<sub>2</sub> hybrid membranes with different dosage of nano-TiO<sub>2</sub>. *Journal of Membrane Science*. 2012;389:522–31.
10. Duranoğlu D. Preparation of TiO<sub>2</sub>/perlite composites by using 23-1 Fractional Factorial Design. *Journal Of The Turkish Chemical Society, Section A: Chemistry*. 2016; 3(3):299-312.
11. Cao X, Ma J, Shi X, Ren Z. Effect of TiO<sub>2</sub> nanoparticle size on the performance of PVDF membrane. *Applied Surface Science*. 2006;253(4):2003–10.
12. Oh SJ, Kim N, Lee YT. Preparation and characterization of PVDF/TiO<sub>2</sub> organic-inorganic composite membranes for fouling resistance improvement. *Journal of Membrane Science*. 2009;345(1–2):13–20.
13. Méricq J-P, Mendret J, Brosillon S, Faur C. High performance PVDF-TiO<sub>2</sub> membranes for water treatment. *Chemical Engineering Science*. 2015;123:283–91.
14. Wei Y, Chu HQ, Dong BZ, Li X, Xia SJ, Qiang ZM. Effect of TiO<sub>2</sub> nanowire addition on PVDF ultra filtration membrane performance. *Desalination*. 2011;272(1–3):90–7.
15. Wang Q, Wang Z, Zhang J, Wang J, Wu Z. Antifouling behaviors of PVDF/nano-TiO<sub>2</sub> composite membranes revealed by surface energetics and quartz crystal microbalance monitoring. *RSC Adv*. 2014;4(82):43590–8.
16. Torlak Y. Polyoxotungstate/oxy-graphene nanocomposite multilayer films for electro catalytic hydrogen evolution. *Journal of the Turkish Chemical Society, Section A: Chemistry*. 2018;
17. Ou X, Pilitsis F, Jiao Y, Zhang Y, Xu S, Jennings M, et al. Hierarchical Fe-ZSM-5/SiC foam catalyst as the foam bed catalytic reactor (FBCR) for catalytic wet peroxide oxidation (CWPO). *Chemical Engineering Journal*. 2019;362(July 2018):53–62.
18. Fadaei A, Salimi A, Mirzataheri M. Structural elucidation of morphology and performance of the PVDF/PEG membrane. *Journal of Polymer Research*. 2014;21(9).
19. Liang W, Luo Y, Song S, Dong X, Yu X. High photo catalytic degradation activity of polyethylene containing polyacrylamide grafted TiO<sub>2</sub>. *Polymer Degradation and Stability*. 2013;98(9):1754–61.
20. Patra N, Salerno M, Malerba M, Cozzoli PD, Athanassiou A. Improvement of thermal stability of poly(methyl methacrylate) by incorporation of colloidal TiO<sub>2</sub> nanorods. *Polymer Degradation and Stability*. 2011;96(7):1377–81.
21. Yang W, Wang H, Zhu X, Lin L. Development and Application of Oxygen Permeable Membrane in Selective Oxidation of Light Alkanes. *Topics in Catalysis*. 2005;35(1–2):155–67.
22. Songur Z, Acar M. Chloromethylation of Polysulfone. *Journal of the Turkish Chemical Society, Section A: Chemistry*. ; 1(1):5.
23. Shi F, Ma J, Wang P, Ma Y. Effect of quenching temperatures on the morphological and crystalline properties of PVDF and PVDF-TiO<sub>2</sub> hybrid membranes. *Journal of the Taiwan Institute of Chemical Engineers*. 2012;43(6):980–8.
24. Li W, Li H, Zhang YM. Preparation and investigation of PVDF/PMMA/TiO<sub>2</sub> composite film. *Journal of Materials Science*. 2009;44(11):2977–84.
25. Dehestaniathar S, Khajelakzay M, Ramezani-Farani M, Ijadpanah-Saravi H. Modified diatomite-supported CuO-TiO<sub>2</sub> composite: Preparation, characterization and catalytic CO oxidation. *Journal of the Taiwan Institute of Chemical Engineers*. Elsevier Ltd.; 2016;58:252–8.
26. Hashino M, Hiram K, Ishigami T, Ohmukai Y, Maruyama T, Kubota N, et al. Effect of kinds of membrane materials on membrane fouling with BSA. *Journal of Membrane Science*. 2011;384(1–2):157–65.
27. Abdelrasoul A, Doan H, Lohi A. Fouling in Membrane Filtration and Remediation Methods. In: *Mass Transfer - Advances in Sustainable Energy and Environment Oriented Numerical Modeling*. 2013.
28. Anvari A, Yancheshme AA, Rekaabdar F, Hemmati M, Tavakolmoghadam M, Safekordi A. Erratum to: PVDF/PAN Blend Membrane: Preparation, Characterization and Fouling Analysis (*J Polym Environ*, (2017), 25, 1348,

- 10.1007/s10924-016-0889-x). *Journal of Polymers and the Environment*. 2017;25(4):1359–60.
29. Gumus H. Performance investigation of Fe<sub>3</sub>O<sub>4</sub> blended poly (vinylidene fluoride) membrane on filtration and benzyl alcohol oxidation: Evaluation of sufficiency for catalytic reactors. *Chinese Journal of Chemical Engineering*. Elsevier B.V.; 2019;27(2):314–21.
30. Mokhtari-Shourijeh Z, Montazerghaem L, Olya ME. Preparation of Porous Nanofibers from Electrospun Polyacrylonitrile/Polyvinylidene Fluoride Composite Nanofibers by Inexpensive Salt Using for Dye Adsorption. *Journal of Polymers and the Environment*. 2018;26(9):3550–63.
31. Shi F, Ma Y, Ma J, Wang P, Sun W. Preparation and characterization of PVDF/TiO<sub>2</sub> hybrid membranes with different dosage of nano-TiO<sub>2</sub>. *Journal of Membrane Science*. 2012;389:522–31.
32. Kubacka A, Ferrer M, Cerrada ML, Serrano C, Sanchez-Chaves M, Fernandez-Garcia M, et al. Boosting TiO<sub>2</sub>-anatase antimicrobial activity: Polymer-oxide thin films. *Applied Catalysis B: Environmental*. 2009;89(3–4):441–7.
33. Attarchi N, Montazer M, Toliyat T. Ag/TiO<sub>2</sub>/ $\gamma$ -CD nano composite: Preparation and photo catalytic properties for methylene blue degradation. *Applied Catalysis A: General*. 2013;467:107–16.
34. He X, Sanders S, Aker WG, Lin Y, Douglas J, Hwang H. Assessing the effects of surface-bound humic acid on the phototoxicity of anatase and rutile TiO<sub>2</sub> nanoparticles in vitro. *Journal of Environmental Sciences*. 2015;2:50–60.
35. García-Fernández L, García-Payo MC, Khayet M. Effects of mixed solvents on the structural morphology and membrane distillation performance of PVDF-HFP hollow fiber membranes. *Journal of Membrane Science*. 2014;
36. J. L. Falconer, K. A. Magrini-Bair. Photo catalytic and Thermal Catalytic Oxidation of Acetaldehyde on Pt/TiO<sub>2</sub>. *Journal of Catalysis*. 1998;179:171–8.
37. Figoli A, Simone S, Criscuoli A, Al-Jilil SA, Al Shabouna FS, Al-Romaih HS, et al. Hollow fibers for seawater desalination from blends of PVDF with different molecular weights: Morphology, properties and VMD performance. *Polymer*. Elsevier Ltd; 2014;55(6):1296–306.
38. Sánchez-Jiménez PE, Criado JM, Pérez-Maqueda LA. Kissinger kinetic analysis of data obtained under different heating schedules. *Journal of Thermal Analysis and Calorimetry*. 2008;
39. Saleh TA, Gupta VK. Synthesis and characterization of alumina nano-particles polyamide membrane with enhanced flux rejection performance. *Separation and Purification Technology*. 2012;
40. Molinari R, Poerio T. Preparation, characterisation and testing of catalytic polymeric membranes in the oxidation of benzene to phenol. *Applied Catalysis A: General*. 2009;358(2):119–128.
41. Zhu Y, Wang B, Wang H, Liu X, Licht S. Towards efficient solar STEP synthesis of benzoic acid: Role of graphite electrode. *Solar Energy*. Elsevier Ltd; 2015;113:303–12.

